

Atmospheric tomography with Rayleigh laser beacons for correction of wide fields and 30 m class telescopes

Roger Angel and Michael Lloyd-Hart
Steward Observatory, The University of Arizona, Tucson, AZ 85721

ABSTRACT

Single sodium beacons will likely be the most convenient for adaptive systems to correct 6-10 m class telescopes over a small field of view (the isoplanatic angle), provided reliable, powerful 589 nm lasers become available and affordable. However, when adaptive optics are applied to extended fields of view and correction of telescopes as large as 32 m diameter, it seems likely that laser beacons produced by Rayleigh scattering will be preferred. For these more demanding applications which require atmospheric tomography, Rayleigh beacons come into their own for two reasons. First, the cone effect, which causes the high turbulence to be sampled at a different scale, is no longer problematic when multiple lasers are used and height dependence is solved for explicitly. Second, the tomographic solution can make use of the beacon created by a laser pulse during all of its journey through the upper atmosphere, not just scattering from a thin layer selected by range gating. In this way a laser that costs an order of magnitude less to buy and maintain than a sodium laser of the same power can yield a brighter beacon and more information about the atmospheric turbulence. This is important because both the number and brightness of beacons or stars must increase with the number of layers included in the tomographic solution. For the same reason, tomography with natural stars is unlikely to be valuable for very large telescopes because in general the number and required brightness of each star increase with corrected field angle, while current narrow-field adaptive optics systems relying on natural stars are already very limited in sky coverage.

Our method for tomography to take advantage of Rayleigh scattering over a wide range of heights uses short pulses from near diffraction-limited, ultraviolet lasers, projected from a small aperture above the telescope's secondary mirror. Each pulse subtends less than 1 arcsec at any instant as it travels up through many kilometers. An imaging detector at the main telescope focus conjugate to mid-height is used to record fast movies of the rising pulses as they come into and out of focus. Phase diversity analysis of the movies taken together then yields the three-dimensional turbulence of the atmosphere.

Keywords: multi-conjugate adaptive optics, laser beacons, very large telescopes, atmospheric tomography

1. COMPARISON OF RAYLEIGH AND SODIUM BEACONS

1.1 General characteristics and difficulties

Rayleigh beacons have been tested and used successfully in a number of adaptive optics systems.^{1,2} Correction to the diffraction limit has been obtained even at optical wavelengths, for example in the images in H α of the Orion nebula obtained by Fugate et al. with the 1.5 m SOR telescope. Nevertheless, Rayleigh beacons are currently out of favor, for a number of reasons. In the past, the powerful lasers they required were typically of rather poor beam quality. Large beam expansion was then required to create seeing limited beacons, typically obtained by projection through the full 1.5 - 2.5 m aperture of the same telescope being corrected. Complex systems for time sharing by switching the main aperture from projection to detection were necessary. To avoid blurring, the scattered return from short projected pulses was detected through a range gate to accept light from only the height at which the projected pulse was in focus

In addition to these operational complexities and flux limitations, the strong cone effect for Rayleigh sources has led to the general belief that higher sodium beacons are to be much preferred, especially for large aperture telescopes. But sodium beacon systems have proven to be very challenging. Foremost among the problems are the extraordinary demands placed on a laser to create an effective beacon. The frequency must be held precisely in tune, ideally at the strongest hyperfine structure component of the 589.0 nm D₂ line, with homogeneous broadening matched to the atmospheric Doppler broadening to minimize saturation. Continuous wave or a high duty cycle pulsed format is preferred, also to avoid saturation. The strong variability of the sodium column density means that high power is needed to ensure an adequate return. The 10 km length of

the scattering column (the thickness of the sodium layer) results in a beacon elongated beyond the seeing limit unless viewed within a few meters from the point of projection. For telescope apertures ≥ 8 m the signal-to-noise ratio of wavefront slope measurements will be significantly degraded because of this effect, even when the laser is launched from the aperture center. Furthermore, the cone effect, though several times less for a sodium beacon compared to Rayleigh, is not negligible. Once apertures ≥ 8 m are used, it will lead to significant degradation in wavefront quality.

1.2 Photon fluxes

For Rayleigh beacons, the atmospheric density and scattering are predictable. We are interested in beacons above 20 km, substantially above the predominant turbulence. To make specific flux comparisons we will assume a beacon wavelength of 351 nm where scattering is strong, but not so strong as to cause heavy attenuation by the lower atmosphere. We assume 25% transmission for the round trip from a telescope at 3 km elevation. Ultraviolet wavelengths 350 - 360 nm are readily available at high power from excimer and frequency tripled neodymium pulsed lasers.

Height (m)	Pressure (mbar)	Return flux (photons/m ² /J)
20,000	55	610,000
21,000	47	470,000
22,000	40	370,000
23,000	35	290,000
24,000	30	230,000
25,000	26	180,000
26,000	22	140,000
27,000	19	120,000
28,000	16	90,000
29,000	14	70,000
30,000	12	60,000
30,000	12	60,000
31,000	10	50,000
32,000	9	40,000
33,000	8	30,000
total		2,800,000

Table 1. Fluxes returned from different heights by Rayleigh scattering over 1 km of a 351 nm, 1 Joule pulse.

Table 1 gives the pressure and returned photon flux for a projected pulse at 351 nm. We have used the lidar equation parameters given by Hardy,³ and the atmospheric properties by Allen.⁴

For a sodium beacon, scattering is by a ~ 10 km thick column at 95 km elevation. For a 1W continuous-wave laser, the measured return for average column density is 840,000 photons/m²/s.⁵ However, the sodium density is quite variable, and is not infrequently found at half the average. Thus a robust system would have to allow for a return as low as 400,000/W/m²/s.

We see that for the same transmitted power, the Rayleigh flux for range gates less than 1 km is less than that for a well-tuned sodium laser scattering from typical sodium density, but if a way can be found to use all the light scattered above 20 km, then the Rayleigh beacon will be several times brighter. When the sodium layer is weak, the Rayleigh total will be nearly an order of magnitude brighter. A launched pulse of 50 mJ at 351 nm will give a return of roughly 140,000 photons/m², the same as the 0.5 – 0.9 μ m flux in 1 ms from a natural star of 5th magnitude.

1.3 Cost and ease of use

Mature laser costs depend strongly on the desired wavelength, spectral purity and pulse format, as well as market and production volume. A reliable 1 kW neodymium YAG laser at 1.06 μ m for welding is probably 1/100 or 1/1000 the cost of a similarly reliable 1 kW laser for isotope separation. We can guess that even mature, mass produced lasers engineered for the strict tuning requirements for sodium will cost an order of magnitude more per watt than existing mass produced lasers suitable for Rayleigh beacons, with no special wavelength or tuning requirement. The complexity of sodium beacon lasers will probably also translate to a similar difference in maintenance and operating costs.

Safety is another issue. Sodium laser beacons operate near the peak of eye sensitivity, and are very highly collimated, so they have diverged only a little even at the height of spacecraft in low earth orbits. They are thus potentially hazardous to aircraft pilots and sensitive satellite cameras. This complicates their use. By contrast, 360 nm beacons are invisible, and do not penetrate aircraft windows. Because they are focused at lower elevation, they also have much weaker fluxes at satellite altitudes.

2. SCATTERING GEOMETRY AND WAVEFRONT SENSING BY PHASE DIVERSITY IN “MOVIE MODE”

2.1 Projecting a sharp beam

Neglecting for the moment the effect of seeing, a diffraction limited gaussian beam brought to a focus with a waist of width $N\lambda$ has a longitudinal depth of focus of $N^2\lambda$.⁶ Let us suppose that a beacon is focused at height h_f and that the beam is projected such that the waist at this height subtends the seeing width, θ_s i.e. $N\lambda/h_f = \theta_s$. Remembering that $\theta_s = \lambda/r_0$ and solving for N , we find for the depth of focus Δh

$$\Delta h = N^2\lambda = \frac{h_f^2\lambda}{r_0^2}. \quad (1)$$

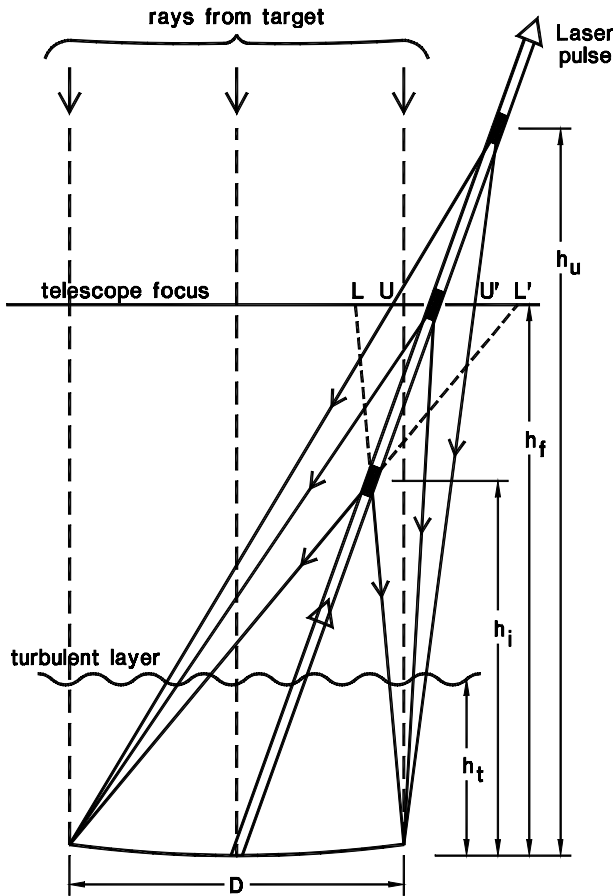


Figure 1. Schematic showing rays from a laser beacon originating from different scattering heights. (Vertical scale greatly compressed)

In this way we eliminate completely the complexity of range gating, and require simply a dichroic mirror to separate the beacon and science wavelengths. The situation for the Rayleigh beacon as it doubles in height is more complex than usual; the images cannot be solved to give a single wavefront because the magnification of the different contributing turbulent layers changes with height, as illustrated in the figure. These effects can, however, be disentangled when a tomographic solution is made.

Because Fried's length r_0 varies as $\lambda^{6/5}$, the greatest depth of field is achieved at shortest wavelength. For a 360 nm Rayleigh beacon at $h_f = 25$ km, subtending 0.6 arcsec in the ultraviolet, appropriate for good seeing, ($r_0(360 \text{ nm}) = 12.4$ cm) we find $\Delta h = 15$ km. The sharp focus thus extends from 17 to 32 km. Such a beam requires a projected gaussian width of 8 cm, and the waist at 25 km is also 8 cm diameter. The rising pulse will subtend less than 1 arcsec from 17 km on up. Since the projected width is less than r_0 , seeing will affect significantly only beam jitter, and short exposures will remain diffraction limited.

The geometry of the scattered beacon rays returning to the main telescope is shown in figure 1. We show rays from a short laser pulse as it rises through heights h_i , h_f and h_u . Phase errors originating in the turbulent layer at height h_i are offset and magnified by an amount that depends on beacon angle and height. The beacon shown is tilted enough so that its returning rays sample turbulence beyond the region traversed by the target rays.

2.2 Phase diversity movie

If the focus of the main telescope were rapidly adjusted for $\sim 100 \mu\text{s}$ to follow the scattering from a short laser pulse as it travels up from 17 to 32 km, a sharp image could be made available for a wavefront sensor. But there is no need to do this to retrieve the wavefront information. We can locate an imaging detector conjugate to fixed height, h_f , equal to say 25 km, and record a 100 μs sequence of short exposures as the images progress through focus. Wavefront aberration causes distortion and brightness variations in the defocused images, which can be used to recover the wavefront aberration by the method of phase diversity.^{7,8}

The spatial resolution of the different phase screens that can be recovered depends on the detail in the defocused images. The angular size of the initial defocused image from height h_i , when the telescope of diameter D is focused at h_f , is $D(h_f - h_i) / h_i h_f$. In figure 1 the defocused image projected to the focal plane conjugate is LL' . Suppose the structure in this image will be seen with resolution of 1 arcsec. Projected to the pupil, this corresponds to a resolution of $5.10^{-6} h_f h_i / (h_f - h_i)$, independent of telescope aperture. For example, if $h_i = 17$ km and $h_f = 25$ km, the resolution is 0.26 m. The defocused image of a 6.5 m telescope would appear 23 arcsec in diameter, and 2 arcmin for a 32 m telescope. Further discussion of phase retrieval made in this way is given by Lloyd-Hart et al.⁹ in these proceedings.

The simplest way to obtain the movie will be to use a mosaic of abutting, fast, imaging detectors at the 25 km image plane, each one dedicated to a single beacon. The number of beacons that can be fitted in will then depend on the size of the defocused images, and hence the height range. For an on-axis ring of six beacons each tilted as shown in figure 1, LL' must be $\leq D/2$, and hence $h_i > h_f/2$. For 19 beacons in all, 12 as shown in figure 1 plus an inner ring of six, LL' must be $\leq D/4$. In this case, $h_i \sim 4/5 h_f$, and $h_u \sim 5/4 h_f$. The total range of height is thus $0.45 h_f$ and would range from 20 to 31 km for $h_f = 25$ km. For a 32 m telescope, the image of all 19 beacons formed at $f/2.5$ would be 125 mm in diameter, and the individual (hexagonal) detectors would be 25 mm across. If more than 19 beacons are needed, then some arrangement would be needed to prevent overlap of the beacon images. Either the height range would need to be restricted, or additional beacons could be interleaved at a slightly different wavelength. A single sharp dichroic beamsplitter would then be used to send light from the two sets of beacons to two separate detector arrays.

2.3 Detector requirements for 32 m telescope tomography.

Imaging detectors with high quantum efficiency and speed will be needed. The most demanding application will be for tomography with a 32 m telescope, when the 2 arcminute images at the extremes of defocus must be sampled with pixels of ~ 0.5 arcsec. For the 19 beacon case, a 256×256 detector will thus be needed to record each one. We anticipate recording the 100 μ s movie in 100 frames, the exposure times varying to ensure that radial blurring of the images is no more than the seeing. The integration time would thus vary from 0.5 μ s at the beginning of the sequence when the images size is changing most rapidly, and lengthen to 2 μ s at the end when blurring is less important, partially offsetting the lower return flux. The expected average number of photons per pixel drops throughout the 100 frame sequence because of reduced air density (table 1). Nevertheless, given the expected return from a 50 W laser, the average number of photons per illuminated pixel does not drop below 20, even for the last and faintest image, so we will always be comfortably in the photon noise limited domain.

Fast detectors with very low noise are now being introduced, for example the CCD60 from Marconi Applied Technologies UK (formerly EEV), can already provide 16 Mpixels/s at $< 1e^-$ rms read noise. Further evolution will be required to record the very fast movie. We imagine that the detector could be made as a 2-dimensional array of 100 μ m photodiodes, each of which is read out at an average 1 MHz rate into its own 100-pixel deep shift register below. After the movie is recorded, the shift registers would be clocked out at ~ 100 kHz rate through A/D converters to output lines. The data rate from each array is < 10 Gbyte/sec, and might be multiplexed on-chip to a single fiber output for each beacon.

2.4 Laser requirements for 32 m telescope beacons

To avoid blur in the Rayleigh movie, both the laser pulse length and the detector exposure time must not be too long. For a 32 m telescope, the pulse length should be ≤ 300 ns, easily accomplished with a Q-switched laser. The rate should be ~ 1000 Hz, slow for an efficient neodymium YAG laser but manageable with YLF.

It is instructive to see how sodium beacons might be used with a 32 m telescope. The scattering takes place in the sodium layer over a range of heights from 90-100 km. The defocus for heights $h_i = 90$ km and $h_f = 95$ km is 4 arcsec. This is not enough defocus to obtain adequate resolution by the phase diversity movie method. But for Shack-Hartmann or equivalent sensors it will be too much. One would then either have to refocus the beacon image on the fly or to gate each pulse into a series of wavefront sensors conjugated to different heights within the 10 km layer. To avoid saturation, the laser pulses should be as long as possible, but must be restricted to $\leq 3 \mu$ s to avoid blurring. They should also come as fast as possible, i.e. a new pulse starting up through the sodium layer as soon as the previous one clears and the telescope can be refocused, an interval of $\sim 50 \mu$ s and a duty cycle of 6%. The implied laser pulse rate, 20 kHz, is fast but could be achievable with some loss of efficiency with a YAG pump. The 3 μ s pulse length is long. Lasers currently under development for sodium beacons do not satisfy these requirements and may thus be of little use for very large telescopes, but this will not be important if, as we expect, Rayleigh beacons are preferred.

3. ATMOSPHERIC TOMOGRAPHY

3.1 How well must we characterize the individual layers for given accuracy of the integrated wavefront?

Let us suppose that the atmosphere is approximated by n discrete thin layers that introduce wavefront distortion, each characterized by the Kolmogorov structure function where the i th layer has Fried length $r_0(i)$. Suppose that the distortion at each layer is specified by phase values given at points separated by distance x on a square grid. In order to calculate the total wavefront distortion in any given direction, it will be necessary to interpolate phase values at arbitrary points on each layer. By analogy to the classic fitting for a deformable mirror with actuators on a square grid, we can say that the mean square error introduced by the interpolation for the i th layer is

$$\Delta_{inter}(i) = 0.34 \left(\frac{x}{r_0(i)} \right)^{5/3}. \quad (2)$$

Let us suppose that the phase values at the grid points are in addition uncertain, with an rms error σ ; then the total mean square error for interpolated points in the i th layer will be

$$\Delta(i) = \Delta_{inter}(i) + \sigma^2. \quad (3)$$

The mean square error for the final wavefront, obtained by summing eq. 3 over the n layers is

$$\Delta = 0.34 x^{5/3} \sum_1^n r_0(i)^{-5/3} + n \sigma^2 = 0.34 \left(\frac{x}{r_0} \right)^{5/3} + n \sigma^2, \quad (4)$$

where we have used the fact that Fried's length for the wavefront propagated through all the layers, r_0 , is given by

$$r_0^{-5/3} = \sum_1^n r_0(i)^{-5/3}. \quad (5)$$

Our final expression in eq. 4 is just what we would obtain by representing the atmosphere as a single layer sampled with the same grid spacing x , but mean square uncertainty $\sigma^2(total)$ in the measured phases that is n times $\sigma^2(layer)$. In other words, for the same total accuracy in the tomographic solution, we need to know the contributing phase screens on as fine a grid as the integrated atmosphere, but the mean square uncertainty at each point needs to be n times better.

3.2 Photon noise and star brightness

In principle the information needed to make a tomographic solution for n layers can be derived from n natural or laser stars, at least for the common atmospheric volume traversed by light from all the stars to the telescope. Compared to the case of measurement of the integrated wavefront by a single star, however, we must measure n times as many independent variables, each with higher accuracy. Each of the n beacons or stars must be n times brighter, based on photon noise considerations.

Suppose we wish to measure the wavefront to an accuracy that will result in Strehl ratio S . For $S < 1$ it follows from the Maréchal approximation that $\Delta = 1-S$. Giving equal weight to the interpolation and grid point error terms, we find that $x = 1.26 r_0 (1-S)^{3/5}$, $\sigma(total) = \sqrt{\{(1-S)/2\}}$ and $\sigma = \sqrt{\{(1-S)/2n\}}$. For an idealized wavefront sensor the phase error in radians is equal to $1/\sqrt{N}$, where N is the number of photons available per estimated phase value. In this limit the theoretical minimum photon flux per unit area per exposure time, assuming ideal quantum efficiency and no losses, is

$$\phi = \frac{1.26n}{r_0^2 (1-S)^{11/5}}. \quad (6)$$

For example, suppose a Strehl of 70% for the measured wavefront is required, r_0 at the wavelength to be corrected is 20 cm, and a 5 layer tomographic solution is to be made. The grid spacing should be 12 cm, and the ideal minimum detected photon flux for each of 5 stars or beacons from each pulse 2200/m² or ~30 per grid point. According to our estimates in section 1, a 1 mJ pulse at 351 nm would suffice. In practice, the movie would be ~ 100 frames long, and to overcome detector read noise and to allow room in the error budget for other sources of error, we may want 10 photons per phase value per frame. A flux

of $\sim 20,000/\text{m}^2$ thus seems more appropriate. To take care also of losses in the projector and receiver optics, and detector quantum efficiency, we may end up wanting a laser pulse of 50 mJ. Such laser powers, amounting to 50W even at 1 kHz rate, are available with frequency tripled YAG systems

3.3 Tomography with a few discrete layers

In a favorable case, nearly all the turbulence may be localized in just a few layers. If there are just three, for example, then three stars are needed to obtain a tomographic solution, each a magnitude brighter than the single star case.

The sky area available for natural stars traversing the common volume is limited to a diameter of less than D/h_t , where D is the telescope diameter and h_t the height of the highest contributing layer. For 6 - 10 m telescopes and $h_t = 10$ km, the field diameter is a few arc minutes. Since field increases with telescope diameter, natural stars may provide the solution for tomography for very large telescopes, provided the layers are thin and few.

The case of a few discrete layers is also favorable for tomography with laser beacons. Because of their conical beam, Rayleigh beacons do not sample as large a volume as natural stars, and the off-axis angle of the least favorable beacon rays (those crossing the full width of the mirror) will be twice the off-axis angle of the beacon. More Rayleigh beacons than natural stars will thus be needed. For a laser at twice the height of the highest turbulence, four times the number of Rayleigh beacons as natural stars will provide the same sampling of the highest layer, with better sampling of lower layers. But they have the advantage that they can be optimally positioned on the sky to obtain the desired sampling, and more can be added as necessary. Because they need not be far separated in angle, the layers need not be very thin for the small number approximation to work.

3.4 Atmosphere with turbulence uniformly distributed in height.

Here we consider the case in which the turbulence is sufficiently broadly distributed that it cannot be well approximated by a few distinct layers. We can still solve as though there were such layers, but their separation must be by no more than r_0/θ , where θ is the off-axis angle of the probing rays. It follows that the number of layers must then be $h_t\theta/r_0$. The minimum number of natural stars to obtain a solution is equal to the number of layers. For an off-axis angle of 2 arcmin (field angle of 4 arcmin, with $r_0 = 0.5$ m and $h_t = 10,000$), it follows that $n = 12$. The situation is now less favorable for natural stars with very large telescopes. Both the number of required stars and their brightness are proportional to field angle. One cannot simply look further afield to find more stars, because the integrated brightness of starlight is on average proportional to solid angle. There is then no advantage for large aperture and field, and one must instead rely on laser beacons.

3.5 Use of tomography in closed loop adaptive optics systems

Atmospheric tomography resolves the atmospheric aberration into different vertical layers. Conventionally, one thinks of using this information to control a multi-conjugate adaptive optics system in which multiple cascaded deformable elements are used to extend the isoplanatic field. Even in single conjugate systems though, tomography has potential application. The simplest use of multiple Rayleigh beacons would be to isolate the contribution of the ground layer, which can be well corrected by an adaptive secondary, typically conjugate to about 100 m below the ground. In this case the seeing over a relatively large field of ~ 10 arcmin would be uniformly improved. The control loop would be used to adjust the secondary so as to minimize the computed ground layer aberration while leaving the other layers alone.

Another use also requiring just one deformable mirror is the correction of a single target, by integrating the aberration in that direction.¹⁰ In this mode, multiple Rayleigh beacons would perform essentially the same wavefront measurement function as a single sodium laser. In contrast to the case with the sodium laser however, the optimal correction for the target would not fully correct the images from any of the beacon lasers themselves because of the cone effect and tilt anisoplanatism contributed by the upper layers. In a significant departure from normal adaptive optics practice therefore, the control loop would not be driving the wavefront sensor error signals to null.

If the target object is too faint or too extended to be used to measure the overall wavefront tilt, a field star will be required. The accuracy of the tilt measurement can be enormously increased if the star's image is also corrected.¹¹ This can be done over an extended field with the addition of a second deformable mirror, placed not in the common path, but only in the natural star channel. In this case, the normal corrections would be sent to the first, common mirror, such as an adaptive secondary,

while the tomography would be used to compute the differential wavefront, which would be sent to the additional mirror. In this way, adaptive optics correction in the near infrared should be possible for faint objects anywhere in the sky. The increased field will include bright enough reference field stars, even at the galactic poles.

The tomographic solution provided by Rayleigh beacons can of course be used for full multi-conjugate adaptive optics, with deformable mirrors conjugate to each layer of the solution. In this case, the beacon wavefronts will be largely corrected, with some additional residual error because of small chromatic differences between the laser and science wavelengths.

4. CONCLUSIONS

Rayleigh beacons sensed by phase diversity look very promising for atmospheric tomography, particularly for the recovery of diffraction limited images by 30 m class telescopes. The sky cover should be much better than for natural stars. Lasers well suited for Rayleigh beacons already exist; reliable sodium lasers with the appropriate pulse format do not yet exist and will likely be much more expensive. In ongoing work we are developing the detector needed for a fast framing, high efficiency camera, planning to make tests at the 6.5 m MMT and modeling in detail the process of tomographic recovery. The real-time computational requirements for tomography are high, but we anticipate they may become sufficiently tractable that Rayleigh beacon tomography could become the preferred solution even for single 6.5 – 10 m telescopes.

ACKNOWLEDGEMENTS

We wish to thank Piero Salinari for valuable discussions when we first recognized the potential of Rayleigh beacons for tomography. Thanks also to Roberto Ragazzoni for stimulating our analysis of the measurement accuracy. This work is supported by the Air Force Office of Scientific Research under grant number F49620-99-1-0285.

REFERENCES

1. R. Q. Fugate, B. L. Ellerbroek, C. H. Higgins, M. P. Jelonek, W. J. Lange, A. C. Slavin, *et al.*, 1994 “Two generations of laser-guide-star adaptive optics experiments at the Starfire Optical Range” *JOSA A*, **11**, 310-324
2. L. A. Thompson and R. M. Castle, 1992, “Experimental demonstration of a Rayleigh scattered laser guide star at 351 nm”, *Optics Letters*, **17**, 1485
3. J. W. Hardy, 1998, *Adaptive Optics for Astronomical Telescopes*, Oxford University Press, 222
4. C. W. Allen, 1973, *Astrophysical Quantities*, Athlone press
5. J. Ge, B. P. Jacobsen, J. R. P. Angel, P. C. McGuire, T. Roberts, B. McLeod, and M. Lloyd-Hart, 1998, “Simultaneous measurements of sodium column density and laser guide star brightness,” *SPIE Proc. Adaptive Optical System Technologies*, **3353**, 242
6. A. E. Siegman, 1986, *Lasers*, University Science Books, 677
7. R. A. Gonsalves, 1982, “Phase retrieval and diversity in adaptive optics,” *Opt. Eng.*, **21**, 829
8. R. G. Paxman, T. J. Schulz, and J. R. Fienup, 1992, “Joint estimation of object and aberrations by using phase diversity,” *JOSA A*, **9**, 1072
9. M. Lloyd-Hart, S. M. Jefferies, E. K. Hege, and J. R. P. Angel, 2000, “New approach to Rayleigh guide beacons,” *SPIE Proc. Adaptive Optical System Technology*, **4007**
10. R. Ragazzoni, E. Marchetti, and G. Valente, 2000, “Adaptive-optics corrections available for the whole sky,” *Nature*, **403**, 54
11. D. G. Sandler, S. Stahl, J. R. P. Angel, M. Lloyd-Hart, and D. W. McCarthy, 1994, “Adaptive Optics for diffraction-limited infrared imaging with 8 m telescopes,” *JOSA A*, **11**, 925